Experimental studies of the flow of concentrated hard sphere suspensions into a constriction

L Isa[1], R Besseling[1], E R Weeks[2] and W C K Poon[1]

[1]SUPA and School of Physics, The University of Edinburgh, James Clerk Maxwell Building, The King's Buildings, Mayfield Road, Edinburgh EH9 3JZ,UK
[2]Physics Department, Emory University, Atlanta, GA, USA

E-mail: `Lucio.Isa@ph.ed.ac.uk`

Abstract. Interesting flow properties are observed when a concentrated suspension of colloidal particles flows into a geometrical constriction. We present here a description of two different experimental techniques used to study the pressure driven flow of dense suspensions of micron–sized hard spheres into glass capillaries. The first one involves the analysis of the driving pressure during the flow, the other one is based on fast confocal microscopy. Technical details are given, together with a selection of preliminary results.

1. Introduction

The flow of complex fluids (colloids, polymers and surfactant solutions) and other materials into a geometrical constriction is a phenomenon occurring in many technical applications as well as in nature. Our blood goes continuously in and out of blood vessels of different sizes. In some pathologies (e.g. stenosis) the vascular diameter is drastically reduced forcing the blood to flow into a narrowing [1]. When the presence of "particles" (blood cells) is taken into account, the scenario acquires more complexity, and the precise vessel geometry as well as the particle properties (e.g. deformability) play crucial roles [2]. The same problem is frequently encountered in industrial applications, for example, in extrusion processes, in which metal or plastic is shaped by being forced into an orifice. In particular, there is now a good understanding of polymer extrusion [3]. The flow of granular media through constrictions is also ubiquitous, e.g. sand going through the narrowing of an hourglass. As reported in the literature [4, 5] arch–like, stress–bearing structures develop at the narrowing and their regular formation and collapse is responsible for the peculiarities of hourglass flow.

The flow of concentrated colloids through constrictions is also of interest. Here, as in the other materials already mentioned, even an apparently simple scenario holds surprises. For example, it has recently been shown [6] that a suspension sucked into a syringe through a narrow needle may be less concentrated than the bulk. This was interpreted as due to the intermittent jamming of particles at the inlet to the needle. In this work we present a microscopic study of such phenomenon using novel experimental techniques. The paper is structured as follows: we shall first introduce the experimental system and then we move to the description of two different methods for the study of the aforementioned phenomenon, discussing, for each of them, relevant technical details, interesting results and applications. The last section includes final remarks.

2. Materials

The system used in the experiments consists of two different batches of poly–methyl–methacrylate (PMMA) spheres (named ASM 104 and ASM 286) sterically–stabilised by chemically–grafted poly–12–hydroxy stearic acid. Particles in the first batch have a radius of 1.0μm, the ones in the second of 1.5μm (determined respectively by optical and confocal microscopy). Both samples are suspended in a mixture of decahydronaphtalene (decalin) and tetrahydronaphtalene (tetralin) in order to obtain refractive index matching to improve the quality of microscope imaging. Particles ASM 286 are also dyed with a fluorophore (NBD, 4 chloro–7 nitrobenz–2 oxa 1,3 diazole). They fluoresce under laser illumination (488 nm) in a confocal microscope. The volume fractions $\Phi = (4/3)\pi R^3 N/V$ (where R is the radius of the N particles in volume V) of different samples are calculated relative to the volume fraction of the sediments obtained by centrifuging the suspensions, which we assume to have $\Phi = 0.64$.
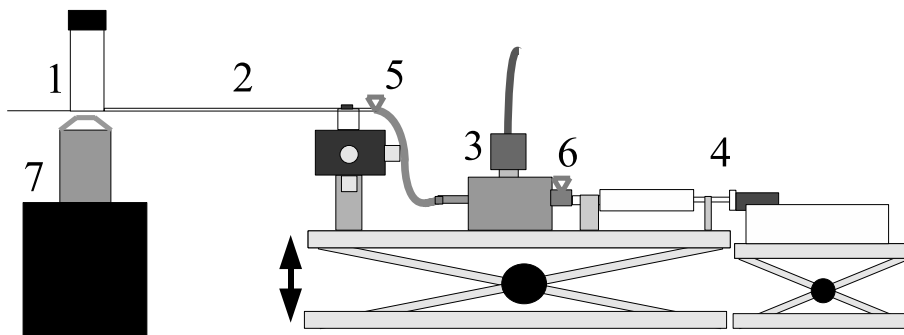

Figure 1. Experimental setup.

3. Pressure experiments

The main idea in the first set of experiments is to deduce the flow properties of a suspension flowing into a cylindrical, millimeter–sized, glass capillary by monitoring how the driving pressure evolves during the flow.

3.1. Experimental method

The apparatus is shown in Figure 1. The suspension to be sucked into the capillary (2), is first loaded into the sample cell (1) while the first valve (5) is closed. By displacing the plunge of a syringe with a motor (4), the pressure downstream from the valve (5) is reduced from atmospheric to P_0, building up an initial driving pressure $\Delta P_0 = P_{atm} - P_0$. The value of the downstream pressure is measured with a pressure gauge (3) (MKS Series 902 Piezo Transducer) through the acquisition of a voltage signal with an I/O card (NI PCI–6014) interfaced with a custom–written Labview program. At this stage the second valve (6) is closed to exclude the syringe volume from the measurement; the measuring volume V_0 is thus given by the sum of the volumes of the pressure gauge, the tubing from (3) to (5) and of the capillary (2). When the first valve (5) is opened again, the suspension starts flowing into a cylindrical glass capillary (2) and the pressure $P(t)$, in a measuring volume $V(t)$, is recorded at a sampling rate of 1000 Hz. The bottom of the sample cell is made of a coverslip, so it is also possible to image simultaneously the flow, in or out of the capillary, with a microscope (7) as will be described in Section 4.

If a newtonian liquid is sucked into the capillary, it can be easily shown that:

$$\frac{P(t)}{P_0} = \frac{P_{atm}}{P_0 + (P_{atm} - P_0)\exp(-t/t_0)} \tag{1}$$

with $t_0 = \dfrac{8\eta L V_0}{\pi a^4 P_{atm}}$, where a is the radius of the capillary, η is the viscosity of the liquid and L is the effective length over which the pressure gradient acts.

In order to derive equation 1 two assumptions have to be made. L is considered constant and the volume change due to the filling up of the capillary is neglected (since it is much smaller than V_0). Such assumptions hold strictly only at short times, while deviations from the predicted trend occur at longer times. Figure 2 (left) shows the calibration measurements obtained using glycerol to find L. The rise of the value of $P(t)/P_0$ corresponds to the pressure recovery in the measuring chamber due to the progressive filling up of the capillary. The measurement ends when the capillary is completely filled up, valve (5) is closed again and therefore the pressure then remains constant. If we plot the time necessary for the glycerol to fill up the capillary (t_{fill}) as a function of ΔP_0 (Figure 2 (right)), we observe the expected behaviour for a Newtonian liquid. As the driving pressure increases, the flow velocity increases as well. Therefore t_{fill} decreases with increasing ΔP_0.
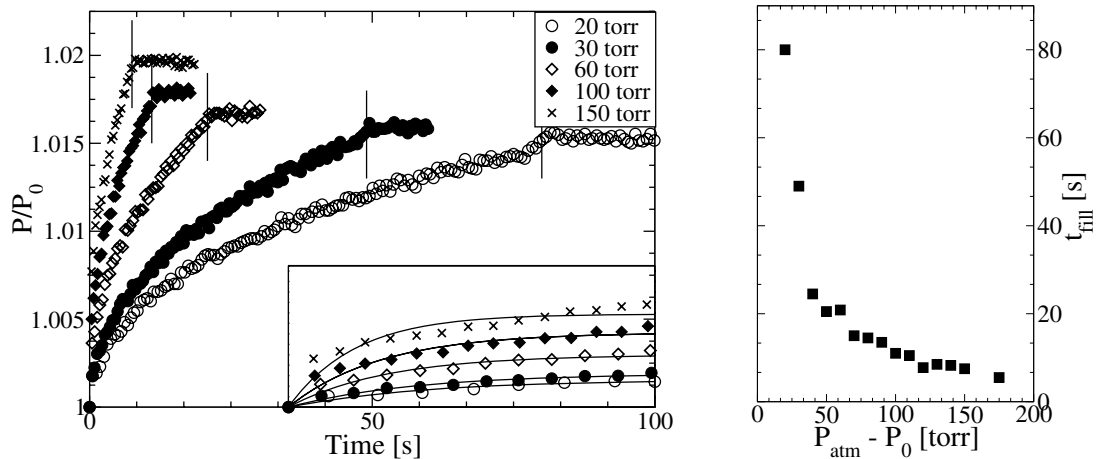

Figure 2. Calibration measurements with glycerol. Left: pressure signals as function of time. The applied pressure differences ΔP_0 are reported in the legend. All the curves start from 1, but some early–time data points have been omitted for clarity. The flattening of the signals corresponds to the end of the measurement, i.e. when the capillary is completely filled with glycerol. The position of the vertical segments indicates the values of t_{fill}. Inset: first $5s$ of the signals and fits from equation 1. Right: t_{fill} as a function of ΔP_0. The data are fitted with the expression reported in the legend.

3.2. Results and discussion

The behaviour mentioned above for a simple liquid, drastically changes when the flowing system is a dense suspension of colloidal hard spheres with a volume fraction above 50%. Figure 3 (left) reports the pressure signals for a suspension of batch ASM 104 with $\Phi = 0.53$. If we look at the values of t_{fill} for this system (Figure 3 (right)), it is evident that a major change has occurred. Not only the inverse proportionality with ΔP_0 is lost, but now the curve is not even monotonic any longer. For low driving pressures, increasing the driving force resolves in

a faster flow (compare curve (∘ 30 torr) and curve (■ 50 torr)), but when ΔP_0 is increased above a certain value (50 torr $< \Delta P_0 <$ 60 torr), increasing it further leads to a slowing down of the flow (see curve □ 60 torr and ● 70 torr). In other words the harder we try to drag the suspension inside the capillary, the more slowly it flows. The non–monotonicity of t_{fill} indicates that a change in the flow behaviour has occurred. In particular from optical microscopy [6] and from direct visual observation, for high driving pressures, the flow becomes irregular and even intermittent. The flow discontinuities are believed to be the cause of the overall slowing down and in the next section we shall describe an experimental technique that is able to give quantitative information on such flow irregularities (data not presented here).
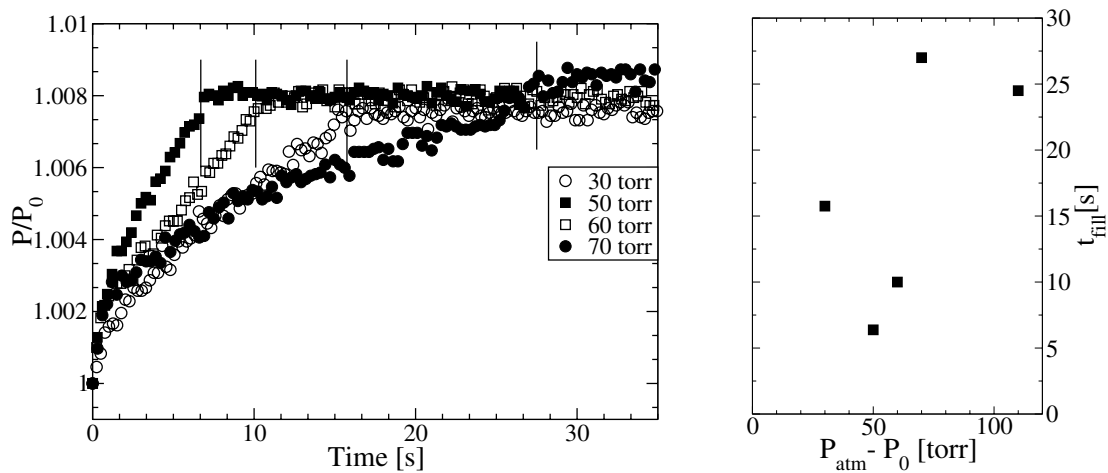

Figure 3. Left: pressure signals for ASM 104 at 53% volume fraction for different driving pressures (see legend). Right: t_{fill} as function of ΔP_0. The non–monotonic behaviour is evident.

4. Confocal imaging

The second technique is based on performing confocal microscopy on the flowing suspension. To obtain a higher image quality we chose to acquire the images inside the capillary (in this case with a rectangular cross section). The high frame rate acquisition of our instrument (Visitech VTeye) allows us to follow the motion of the single particles during the flow and therefore to collect information on their individual positions and velocities.

4.1. Experimental method

Confocal microscopy has now become a well–established method of studying the dynamical and structural properties of dense colloidal systems (e.g. in [7, 8]). The key advance consists in the possibility of imaging deep in the sample, obtaining the coordinates of the particles' centres in each image (see Figure 4) and then tracking them frame by frame. Further information on the procedure for quiescent suspensions can be found in [9]. Here we shall focus on the particular innovations needed to analyse flow experiments. The first step is the *pre–tracking*; a software routine finds the position of the centre of each particle according to the intensity profile of the emitted fluorescent light. Once the coordinates of the centres have been found in each frame, the *tracking* procedure merges them into trajectories describing the particles motion in the *xy* focal plane; each particle is labelled with an identification tag and the tracking routine looks for particles that can be assigned the same tag within a tracking range in the following frame. One of the assumptions which make the procedure work is that the frame by frame displacements are sufficiently small so that the combinatorics associated with following particles' trajectories are
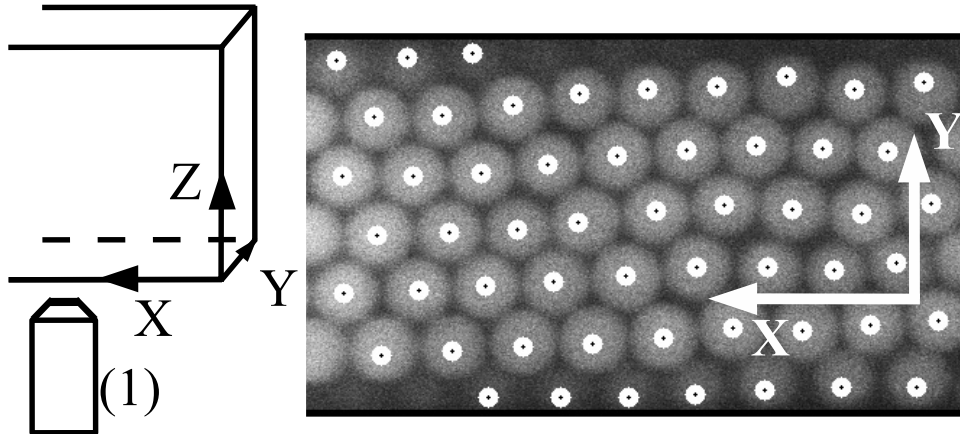
Figure 4. Left: sketch of the experiment geometry. x is the direction of flow, y is the transverse direction and z indicates the depth. 2D images of a xy plane of the capillary are collected with a confocal microscope (1), imaging from below. The usual sampling rate is 87 frames per second. Right: confocal image of the first layer (cross section 35μm $\times$ 20μm) of a dense suspension of ASM 286 (particle diameter 3 μm) inside a 20μm $\times$ 200μm glass capillary. The presence of the capillary wall induces a crystalline layer. The white circles and the black dots represent the particles' centres as found by the pre–tracking procedure.

limited. Given the position for a particle in the first frame, and all the possible new positions within a certain range in the second frame, the procedure considers all possible identifications of the old position with the new ones, and chooses that identification which results in the minimal squared displacement. Figure 5(a) shows a histogram of the frame by frame displacements in the x (flow) and y (transverse) direction for a typical flow experiment. We notice that the y histogram nicely decays within the tracking boundaries (i.e. the identified y displacements are limited and inside the tracking range, thus the transverse motion of the particles is accurately tracked) but the one in the x direction is ill behaved. Due to the flow, the particles are moving too far to be tracked successfully and many of them move out of the tracking range. In order to perform the tracking effectively, we need to find a way to remove the advective motion and follow the particles in a co–moving frame, so that also the x displacements are limited.

The procedure that we developed is based on the correlation between two consecutive images. Let $I_1(x,y)$ and $I_2(x,y)$ be the intensity patterns at position (x,y) in the first and the second image. Image 2 is shifted back by a certain number of pixels $(\Delta x, \Delta y)$ and the correlation coefficient

$$c = \frac{cov[I_1(x,y)I_2(x-\Delta x, y-\Delta y)]}{\sqrt{var[I_1(x,y)]var[I_2(x,y)]}} \qquad (2)$$

is computed for each shift within a desired range and this procedure is repeated for different $(\Delta x, \Delta y)$, until c is maximised. The values of the frame by frame shifts are then subtracted from the particles coordinates in order to have them in a co–moving reference frame. The geometry of our experiments has further consequences on the implementation of this method. Firstly, the flow is exclusively in the x direction, so only horizontal shifts are considered. Secondly, the procedure cannot be performed straight away on the whole images because the flow velocity varies with y, i.e. the flow profile is not uniform and so maximising the correlation only relates to an average motion. However, this problem can be overcome if we examine the positions of the
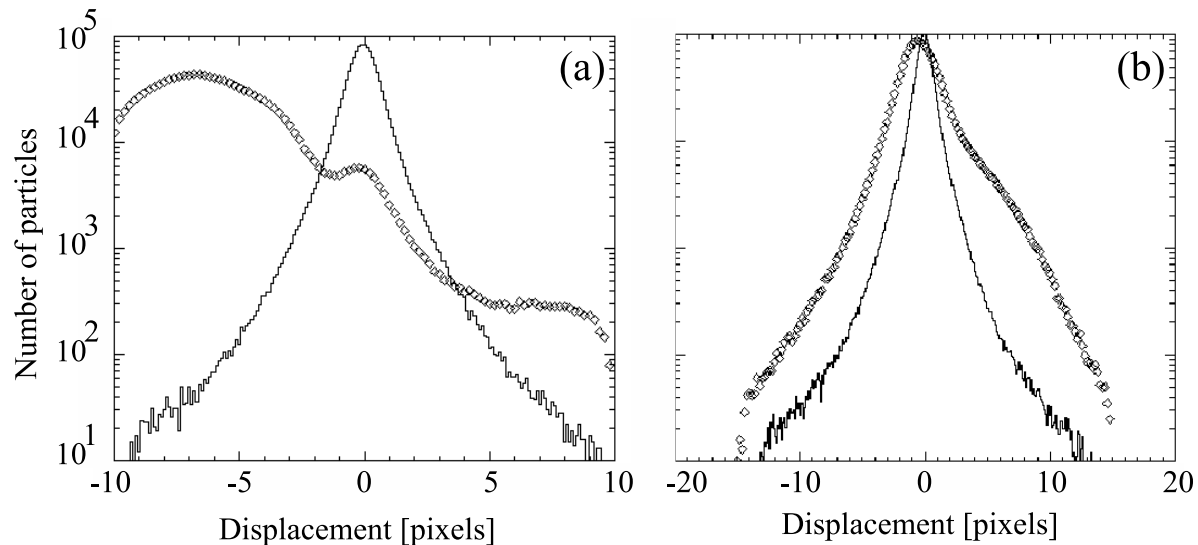
Figure 5. Histograms of x ($\Diamond$) and y ($-$) displacements after 8000 frames for a typical experiment in the laboratory reference frame before (a) and in the the co–moving reference frame after (b) the advection removal procedure. The y displacements are always smaller as the flow is along x. The histograms show the number of particles which centre moves a certain number of pixels within two consecutive frames.

particles inside the capillary as obtained by the pre–tracking. Figure 6 shows a histogram of the y coordinates from 8000 frames in a typical flow experiment. It is evident that the particles are arranged in well–defined horizontal layers. The presence of layering makes the image correlation much easier despite the y–dependent flow profile. The images can now be divided into y–bins corresponding to layers and the correlation procedure can be run separately on each of them; within each layer the value of c is averaged over x and y. Once all the values for the different y–bins have been obtained, they are merged together to create a velocity profile to be subtracted from the particles' coordinates to have them in a y–dependent co–moving frame of reference. This image correlation procedure is however not able to eliminate completely the advective motion, especially in the central part of the capillary where the layering is not as defined as at the edges. A second advection removal is therefore necessary, but because now the main non–uniformity has already been cancelled, removing an averaged flow proves to be effective enough. By tracking the particles after the non–uniform advection removal we can compute the average of the frame by frame displacements. Subtracting this from the previously corrected coordinates we obtain thus a new set of values in a truly co–moving reference frame. Figure 5 (b) shows the histograms of the x and y displacements in the co–moving reference frame obtained when performing the tracking after the two–steps advection removal procedure described above. We now notice that the x histogram falls well within the tracking range. Finally, adding the total motion back to the coordinates allows us to move back to the laboratory frame of reference and to study the flow following each particle's trajectory.

4.2. Results and discussion

As a first application of the procedure described above we have looked at the velocity profiles of ASM 286 suspensions into rectangular capillaries with an aperture of 40μm $\times$ 400μm at a depth of 15μm for two different volume fractions (see Figure 7). When the suspension is fairly dilute

($\Phi \sim 30\%$), a parabolic profile is observed as expected form a Newtonian liquid undergoing Poiseuille flow (also refer to [10]). For a dense suspension with $\Phi \sim 0.64$, the shape of the velocity profile changes considerably. We still observe that particles close to the capillary walls are subjected to shear, in other words, different layers of particles move with different velocities, but in the center of the capillary a quite extended plug of nearly un–sheared suspension is found. Particles in this region basically move all with the same speed and are rarely found to exchange neighbours, resembling closely what observed in the case of vertical granular chute flows[11].

This represents just a first proof of the effectiveness of particle tracking combined with the non–uniform advection removal technique and future work points towards the use of such technique for the study of intermittent flow at a microscopic level.
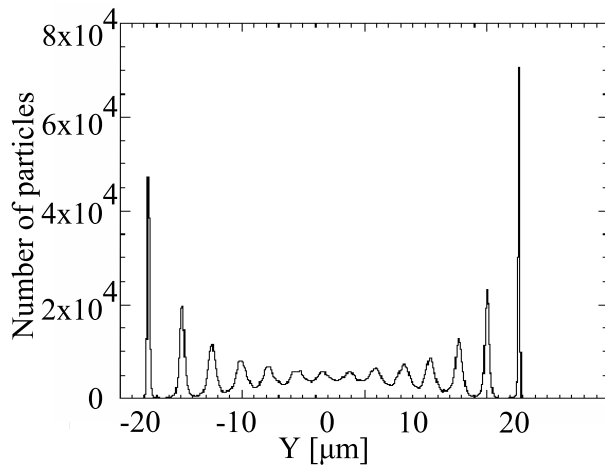

Figure 6. Histogram of the y positions inside a $40\mu m \times 400\mu m$ capillary obtained after 8000 images in a typical experiment. The images are taken at a depth of 15 μm in the capillary. 14 layers can be identified and the ones at the edges of the capillary are better defined.
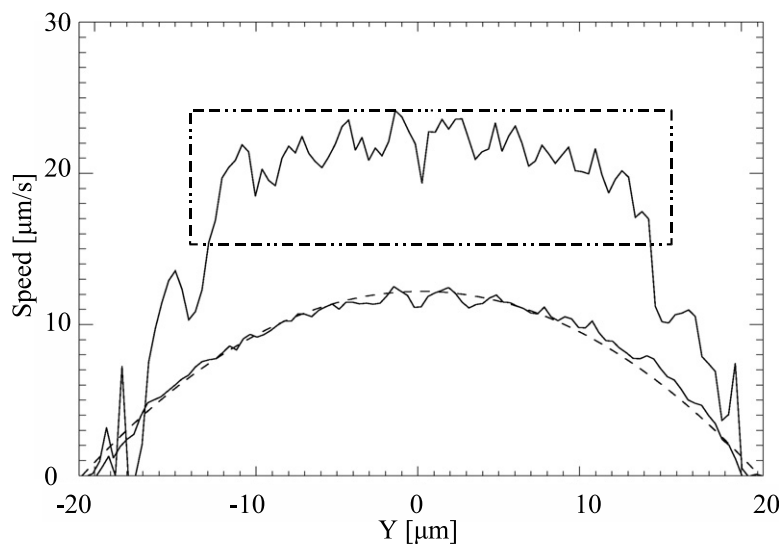

Figure 7. Average flow profiles for a 30% volume fraction ASM 286 suspension (bottom curve, 5000 frames) and for a ASM 286 sediment (top curve, 5000 frames). For the more dilute case the profile is fitted with a parabola (dashed line) as expected for an ideal Poiseuille flow; for the sediment we notice that the shape of the curve changes, showing a nearly un–sheared plug in the center (highlighted by the dashed box) where the particles move all with roughly the same speed. The jaggedness of the line reflects the layering in the dense system.

5. Discussion and future work

We have shown how the techniques described in the previous sections can be applied to the study of flow of dense colloidal suspensions. In relation to the analysis of the pressure signal, as

already hinted before, the applied ΔP_0 plays a fundamental role, determining the flow behaviour of the suspension for a given size of particles and volume fraction: driving pressures above a certain value lead to a slowing down of the flow, in contrast to what observed for a Newtonian liquid. This is not the only non-monotonic trend associated with sheared dense colloidal suspensions. For instance, as reported in the literature [12], the viscosity of concentrated hard spheres suspensions decreases with increasing shear rates for low shear (shear thinning), but rises again for high shear rates (shear thickening) and even starts fluctuating above a certain threshold (discontinuous shear thickening) [13]. Surprisingly, a very similar non–monotonic "flow" behaviour has also been found in simulations of crowd panic [14]. When a crowd escapes from a room through a narrowing, increasing the target speed of individuals leads to a shorter leaving time up to a critical value where the whole process becomes slower.

While the pressure measurements give macroscopic information on how the suspension flows when driven into a constriction, fast confocal microscopy can look at the other end of the spectrum, trying to relate those macroscopic events to microscopic dynamics. With the use of the advection removal procedure described above, the flow velocities inside the capillary can be measured and the presence of fluctuations in those values (flow irregularities) can then be quantified.

To conclude the paper, we believe that the experimental techniques described above can be successfully used as a means of investigating the properties of dense colloidal suspensions flowing into geometrical constrictions and can add useful information to the scenario of non–linear shear phenomena in general.

Acknowledgments

References

[1] D N Ku. Blood flow in arteries. *Annual Review of Fluid Mechanics*, 29:399–434, 1997.

[2] H B Li et al. Lattice boltzmann simulation on particle suspensions in a two–dimensional symmetric stenotic artery. *Physical Review E*, 69(3):031919, 2004.

[3] M W Collis et al. Constriction flows of monodisperse linear entangled polymers: Multiscale modeling and flow visualization. *Journal of Rheology*, 49(2):501–522, 2005.

[4] X-L Wu, K J Måløy, A Hansen, M Ammi, and D Bideau. Why hour glasses tick. *Physical Review Letters*, 71(9):1363–1366, 1993.

[5] B K Muite, M L Hunt, and G G Joseph. The effects of a counter-current interstitial flow on a discharging hourglass. *Physics of Fluids*, 16(9):3415–3425, 2004.

[6] M D Haw. Jamming, two–fluid behaviour and 'self–filtration' in concentrated particulate suspensions. *Physical Review Lettres*, 92:185506, 2004.

[7] E R Weeks, J C Crocker, A C Levitt, A Schofield, and D A Weitz. Three–dimensional direct imaging of structural relaxation near the colloidal glass transition. *Science*, 287:627–631, 2000.

[8] A D Dinsmore, E R Weeks, V Prasad, A C Levitt, and D A Weitz. Three–dimensional confocal microscopy of colloids. *App. Optics*, 40:4152–4159, 2001.

[9] J C Crocker and D G Grier. Methods of digital video microscopy for colloidal studies. *J. Colloid Interface Sci.*, 179:298, 1996.

[10] M Frank, D Anderson, E R Weeks, and J F Morris. Particle migration in pressure–driven flow of a brownian suspension. *J. Fluid Mech.*, 493:363–378, 2003.

[11] O. Pouliquen and R. Gutfraind. Stress fluctuations and shear zones in quasistaic granular chute flows. *Physical Review E*, 53(1):552–561, 1996.

[12] W J Frith, P d'Haene, R Buscall, and J Mewis. Shear thickening in model suspensions of sterically stabilized particles. *Journal of Rheology*, 40(4):531–548, 1996.

[13] V T O'Brien and M E Mackay. Stress components and shear thickening of concentrated hard sphere suspensions. *Langmuir*, 16:7931–7938, 2000.

[14] D Helbing, I Farkas, and T Vicsek. Simulating dynamical features of escape panic. *Nature*, 407:487–490, 2000.